PHYSICAL REVIEW D **79,** 015008 (2009)

Discriminating dark matter candidates using direct detection

G. Bélanger,[1] E. Nezri,[2] and A. Pukhov[3]

[1]*LAPTH, Université de Savoie, CNRS, B.P.110, F-74941 Annecy-le-Vieux, France*
[2]*LAM,CNRS, Université Aix-Marseille I, 2 place le Verrier, 13248 Marseille, France*
[3]*Skobeltsyn Inst. of Nuclear Physics, Moscow State Univ., Moscow 119992, Russia*

(Received 31 October 2008; published 22 January 2009)

We examine the predictions for both the spin-dependent and spin-independent direct detection rates in a variety of new particle physics models with dark matter candidates. We show that a determination of both spin-independent and spin-dependent amplitudes on protons and neutrons can in principle discriminate different candidates of dark matter up to a few ambiguities. We emphasize the importance of making measurements with different spin-dependent sensitive detector materials and the need for significant improvement of the detector sensitivities. Scenarios where exchange of new colored particles contributes significantly to the elastic scattering cross sections are often the most difficult to identify, the LHC should give an indication whether such scenarios are relevant for direct detection.

DOI: 10.1103/PhysRevD.79.015008 PACS numbers: 95.35.+d, 12.60.Jv

I. INTRODUCTION

Unraveling the properties of a new stable cold dark matter (CDM) particle is a challenge for ongoing or future astroparticle and collider experiments. The most convincing evidence for CDM so far is provided by WMAP [1] and SDSS [2]. Their precise determination of the relic density of CDM strongly constrains the parameter space of the various new particle physics models (NP) [3–10]. This single observable, $\Omega_{\rm CDM}h^2$, is however not sufficient to pin down the properties of CDM even when assuming that the candidate is a weakly interacting massive particle, χ. Additional information on the nature of dark matter could also be obtained from measurements of detection rate in different detectors, observations of a signal in photons, antiprotons, positrons, or neutrinos produced after annihilation of dark matter, and discovery and measurements of properties of new particles at colliders.

Several models for new physics containing a CDM candidate have been proposed in the past [11]. The most popular examples of new stable weakly interacting particles at the electroweak scale include the neutralino in supersymmetric models [12,13], right-handed neutrinos [14–16], scalars or vector bosons in extra dimension models [17–19], vector bosons in little Higgs models [20,21], and scalars in extensions of the standard model (SM) [22–24]. Right-handed sneutrinos as a CDM candidate have also been revived lately [25–27]. Predictions for signals in direct [19,28–32], indirect [33–45], or collider experiments have been made within each of these models [7,46–58]. Furthermore, in specific case studies, in particular, within supersymmetric models, the prospects of determining the properties of the new particles and from there infer a ''collider'' prediction for the relic density or for the detection rates were analyzed [47,59–61]. While colliders and, in particular, the LHC have a good potential for discovering and identifying new particles present in various extensions of the standard model, direct detection experiments (DD) will be the ones to provide evidence for a stable relic particle [62,63]. Furthermore, in some cases, direct detection experiments have better discovery prospects than the LHC. The best known example is the so-called focus point region in constrained supersymmetric models [64–66]. We therefore concentrate here on direct detection aspects and consider only models which offer the best detection prospects, those with a weakly interacting particle at the electroweak scale.

A number of experiments are currently searching for CDM by measuring the elastic scattering rate on nuclei in large detectors. Their sensitivity is being improved and upper limits are updated regularly. The best upper limit on the proton-χ spin-independent (SI) cross section has been recently obtained by Xenon, $\sigma^{\rm SI}_{\chi p} < 4.5 \times 10^{-8}$ pb for a CDM of 30 GeV [67] and CDMS, $\sigma^{\rm SI}_{\chi p} < 4.6 \times 10^{-8}$ pb for a CDM of 60 GeV [68]. These limits are already putting constraints on the parameter space of new physics models. Limits on spin-dependent (SD) cross sections are much less restrictive. The best limits are now obtained by KIMS for protons, $\sigma^{\rm SD}_{\chi p} < 1.6 \times 10^{-1}$ pb [69] and by Xenon for neutrons, $\sigma^{\rm SD}_{\chi n} < 6 \times 10^{-3}$ pb [70]. Indirect detection of neutrinos coming from CDM annihilation in the Sun sets a limit on $\sigma^{\rm SD}_{\chi p}$, the best limit is from Super-Kamiokande, $\sigma^{\rm SD}_{\chi p} < 4. \times 10^{-3}$ pb [71]. These do not yet allow us to test the most popular NP models.[1]

One difficulty in extracting precise information from an elastic scattering rate on nuclei is that the rate depends not only on the details of the particle physics model but also large theoretical uncertainties are introduced by the CDM

[1]Note that DAMA/LIBRA have very recently confirmed their annual modulation signal [72]. We will not consider this result as it seems to be incompatible with other searches unless the CDM particle is below 10 GeV [73,74], in the sample models we consider CDM candidates are rather in the 30–1000 GeV range.

velocity distribution, the nuclear form factors and the coefficients that describe the quark content in the nucleon. The former can be eliminated by taking ratios of rates in different materials while a large part of the uncertainty from the quark content in the nucleon will drop out when taking ratios of proton to neutron amplitudes. Fortunately many of the detectors set up or planned use different materials and thus can be sensitive to different combinations of proton and neutron amplitudes. The procedure for extracting in a model-independent way the amplitudes for spin-dependent interactions on protons and neutrons was discussed in [75,76]. The spin-independent interactions on the other hand are basically sensitive to one combination of neutron and proton amplitudes, this is because all heavy materials have roughly the same ratio of protons to neutrons [77]. In this paper our first goal is to make a direct comparison of the predictions for DD rates in a variety of models. Our second goal is to examine the prospects for determining the properties of CDM particles after a signal has been observed. For this we will use directly the event rates or assume that the spin (in)dependent proton and neutron amplitudes have been extracted. For model discrimination we assume that future spin-independent and spin-dependent detectors will have sufficient sensitivity to measure a signal. This could occur in the near future as many models have predictions near the present reach of DM detectors. For this analysis we chose to include a large selection of scenarios in each model and considered all models that could potentially lead to a signal in one of the large detectors being planned, All scenarios where the rates are too low are disregarded. This means that we will consider the maximal achievable sensitivity to be $\sigma^{\rm SI}_{\chi p} \approx 10^{-10}$ pb, for example, with Eureca [78] and $\sigma^{\rm SD}_{\chi p} \approx 4 \times 10^{-7}$ pb, as in the COUPP proposal [79]. Although this last value requires a significant improvement in SD detectors, we emphasize the importance of the SD interactions in determining the properties of the CDM candidate.

Comparative studies of the prospects for direct detection in new physics models have been performed in [80,81]. Recently a comparison of the SI detection rates and rates for indirect detection of neutrinos in the case of the MUED, little Higgs, and MSSM models was presented [82]. The potential of a combined measurement of SI and SD rates to distinguish MUED from MSSM with COUPP using two different materials was also examined [83]. We expand on these analyses in many ways. First we examine a larger class of MSSM models, second we rely heavily on detectors sensitive to SD interactions, and third we insist on the importance of using different materials to extract both the neutron and proton amplitudes. We also take into account uncertainties from the quark coefficients in nucleons and use an improved calculation of the direct detection rate [84]. This is a first step towards a more general analysis where one would combine information from both direct and indirect detection as well as from collider searches, see also [81].

This paper is organized as follows: after setting up our notation in Sec. II, we summarize in Sec. III the predictions for the SI and SD cross sections on nucleons as well as for the ratios of SD and SI amplitudes on protons and neutrons in different CDM models. We consider Majorana fermions (in particular the neutralino in SUSY), a right-handed Dirac neutrino, as well as vector and scalar particles. The results of our scans over the parameter space for each sample models are presented in Sec. IV. We first compare the predictions for SI and SD rates in each of our sample models. We then show which models can in principle be distinguished by measurements of both SI and SD amplitudes on protons and neutrons. The predictions for the event rates on various nuclei are then compared. Finally, we briefly mention the case where a signal can be observed only in the SI interaction. Our results are summarized in Sec. V.

II. DIRECT DETECTION

The total scattering cross section of a DM particle, χ, off a pointlike nucleus for spin-independent interactions reads

$$\sigma_0^{\rm SI} = \frac{4\mu_\chi^2}{\pi}(\lambda_p Z + \lambda_n (A - Z))^2, \tag{1}$$

where $\mu_\chi = m_\chi M_A/(m_\chi + M_A)$ is the reduced χ-nucleus mass and M_A the mass of the nucleus. Te proton(neutron) amplitudes. are related via some coefficients to the amplitudes for χ-quark scattering, λ_q. For example, for scalar interactions of Majorana fermions, in the notation of [84]

$$\lambda_{p,n} = \sum_{q=1,6} f_q^{p,n} \lambda_q, \tag{2}$$

where $f_q^{p,n}$ describes the contribution of quark q to the mass of the nucleon. The quark coefficients for scalar interactions have large uncertainties [85]. To take these into account we vary the input parameters of micrOMEGAs2.2 [84] in the range

$$\sigma_{\pi N} = 55\text{–}73 \text{ MeV} \quad \text{and} \quad \sigma_0 = 35 \pm 5 \text{ MeV}, \tag{3}$$

which in essence amounts to varying the s-quark content in the nucleon in the range $0.19 < f_s^p < 0.56$. The heavy quarks coefficients, f_Q^N, are related to those of the light quarks [86]. In the case of a Dirac fermion with an effective vectorial interaction, the coefficients that describe the quark content in the nucleon just count the number of valence quarks and therefore have no theoretical uncertainty [86].

For spin-dependent interactions, the pointlike nucleus cross section reads

$$\sigma_0^{\rm SD} = \frac{\mu_\chi^2}{16\pi}\frac{J_A + 1}{J_A}(\xi_p S_p^A + \xi_n S_n^A)^2, \tag{4}$$

where J_A is the total spin of the nucleus and $S_{p,n}^A$ are obtained from nuclear calculations. The SD nucleon am-

plitudes, ${\xi_{p,n}}^2$ are related to the quark amplitudes,

$$\xi_{p,n} = \sum_{q=u,d,s} \Delta q^{p,n} \xi_q, \tag{5}$$

where the coefficients $\Delta q^{p,n}$ have been estimated for light quarks [86]

$$\Delta_u^p = 0.842 \pm 0.012; \qquad \Delta_d^p = -0.427 \pm 0.013;$$
$$\Delta_s^p = -0.085 \pm 0.018 \Delta_u^n = \Delta_d^p; \tag{6}$$
$$\Delta_d^n = \Delta_u^p; \qquad \Delta_s^n = \Delta_s^p$$

In the numerical analysis we will allow the coefficients to vary within their 1σ range.

The recoil energy distribution measured in a detector further contains some dependence on the nuclear form factors as well as on the CDM velocity distribution.

$$\frac{dN}{dE} = \frac{2M_{\rm det}t}{\pi} \frac{\rho_0}{m_\chi} [F_A^2(q)(\lambda_p Z + \lambda_n (A - Z))^2 \tag{7}$$

$$+ \frac{4}{2J_A + 1} (S_{00}(q)\xi_0^2 + S_{01}(q)\xi_0\xi_1 + S_{11}(q)\xi_1^2)] I(E), \tag{8}$$

where $\xi_1 = \xi_p + \xi_n$ and $\xi_0 = \xi_p - \xi_n$. $F_A(q)$ is the nuclear form factor for scalar interactions and $S_{ij}(q)$ the form factor for spin-dependent interactions, both depend on the momentum transfer, $q = \sqrt{2M_A E}$ [87]. ρ_0 is the local neutralino density, $M_{\rm det}$ the detector mass and I(E) the integral over the velocity distribution

$$I(E) = \int_{v_{\rm min}}^{\infty} \frac{f(v)}{v} dv, \tag{9}$$

where $v_{\rm min} = (\frac{EM_A}{2\mu_\chi^2})^{1/2}$. To compute the cross sections on nucleons and the event rates we rely on micrOMEGAs2.2 [84].

All information on the CDM model is contained in the amplitudes λ_p, λ_n, ξ_p, ξ_n as well as in the mass of the CDM. Once a signal has been observed, one could use data from different detector materials to extract information on these amplitudes [88]. This evidently necessitates making some assumption about both the halo velocity distribution, the dark matter distribution as well as on the nucleon and nuclear form factors. The dependence on the velocity and on the dark matter distribution however drops out when taking ratios of the nucleon amplitudes. Furthermore, some of the uncertainty from the quark coefficients in the nucleon also drop out. This is because the sea quarks coefficients, which give the dominant contribution, are identical for protons and neutrons.

We choose as independent parameters the ratios ϕ, ξ/λ_+ and λ_+, λ_p/λ_n which characterize the overall SI rate,

$$\xi_p = \xi \sin\phi; \qquad \xi_n = \xi \cos\phi; \qquad \lambda_+ = \lambda_p + 1.4\lambda_n. \tag{10}$$

Note that the factor of 1.4 in λ_+ depends on the ratio of protons to neutrons in the nucleus. Typically this ratio does not vary much [77], our choice gives the maximal sensitivity in heavy nuclei. Nuclei that are sensitive to SD interactions do so primarily through an unpaired nucleon, this means they have either S_p or $S_n \neq 0$ and have little sensitivity to the interference term $\xi_p\xi_n$ in Eq. (4) [89]. The sign of $\phi = \text{atan}(\xi_p/\xi_n)$ is therefore hard to determine.

The mass of the CDM candidate can be determined from the nuclei recoil energies. This works best when $M_\chi \approx$ 100 GeV [90] although a new method to improve the mass determination for a heavy DM particle using signals from two different detectors was proposed recently [91].

III. DM MODELS

We consider a selection of models representative of different CDM candidates in the 30 GeV–1 TeV range: Majorana fermion (the neutralino in the MSSM), Dirac fermion (a right-handed neutrino), gauge boson (the heavy photon in little Higgs models or the B_1 in MUED models), or scalar particles in extended Higgs models. The predictions for the rates for direct detection have been studied in all these models and rates can vary by orders of magnitude within each model [7,11]. For each CDM candidate the dominant process for elastic scattering influences the overall scattering cross section as well as the relations among the proton/neutron amplitudes. We will explore these relations within models representative of each type of CDM. A summary of the different mechanisms for CDM elastic scattering in various models is provided in Table I. Note that two special subclasses of the MSSM have been introduced. The main difference between these two classes is the range of mass of squarks, in MSSMH they are heavy and therefore do not contribute to DD.

A. MSSM

In the MSSM the CDM is a Majorana fermion, the neutralino, χ_1^{0}[3] The nature of the neutralino, whether it is mostly bino or contains a mixture of Higgsino or wino, strongly influences the annihilation mechanisms and the CDM relic density. For direct detection one gets two types of contributions, Higgs and squark exchange for SI interactions and Z and squark exchange for SD interactions. In

[2]Note that our definition of the nucleon amplitudes differs from the usual convention where one uses $a_{p,n} = \sqrt{2}G_F\xi_{p,n}$ [75,86].

[3]We do not consider the case of the sneutrino CDM which usually gives too large detection rate unless its coupling to the Z is suppressed [25,26,92].

TABLE I. Dominant mechanism for CDM-nucleon elastic scattering

Model	CDM	Nature	SI	SD
MSSMH	Neutralino	Majorana fermion	Higgs	Z
MSSMQ	Neutralino	Majorana fermion	Higgs + squark	Z + squark
RHN	ν_R	Dirac fermion	Z + Higgs	Z
MUED	B_1	Vector boson	Higgs + KK quarks	KK quarks
LHM	A_H	Vector boson	Higgs + Quarks	Quarks
IDM	H^0	Scalar	Z + Higgs	

general the Higgs and Z exchanges dominate since the squark contributions suffer from a mass suppression (the squarks are generally at the TeV scale). We will consider two categories of MSSM models. In the first, MSSMH, sfermions are heavy (2 TeV) and do not contribute to DD. In this model CDM annihilation requires a lightest neutralino with some Higgsino or wino component. In the second, MSSMQ, we force one of the squark masses to be $M_{\tilde{q}_{L,R}} < 2M_\chi$. We introduce these classes of models as a way to quantify the impact of the squarks in DD. Note that these two types of MSSM models can be easily distinguished at LHC which can probe the s-quark sector up to more than 2 TeV [63,93]. In both cases we will assume the sleptons to be heavy since sleptons do not contribute to direct detection. However, one should keep in mind that sleptons can contribute to the CDM relic density, both through annihilation or coannihilation, so our analysis is not completely general when confined to models that are in agreement with the measured value for the CDM relic density. Such light sleptons can be searched for at the LHC.

Taking into account the dominant Higgs exchange diagram only, the spin-independent interaction reads

$$\lambda_N = -m_N \frac{g^2}{4M_W c_W} \sum_{i=1,2} [(f_u^N + f_c^N + f_t^N) g_{h_i uu} + (f_d^N + f_s^N + f_b^N) g_{h_i dd}] g_{h_i \chi\chi} \frac{1}{m_{h_i}^2}, \quad (11)$$

where $h_i = h, H$ $g_{huu} = \cos\alpha/\sin\beta$, $g_{hdd} = -\sin\alpha/\cos\beta$, $g_{Huu} = \sin\alpha/\sin\beta$, $g_{Hdd} = \cos\alpha/\cos\beta$, and α is the Higgs mixing angle. In the decoupling limit, at large M_H, $\sin\alpha = -\cos\beta$. The SUSY-QCD corrections can shift the Higgs couplings to down-type quarks, especially at large values of $\tan\beta$. These corrections are taken into account in the numerical analysis but for simplicity will be omitted from the discussion here. The couplings of the light Higgs to χ_1^0 reads

$$g_{h\chi\chi} = (\cos\alpha Z_{14} + \sin\alpha Z_{13})(c_W Z_{12} - s_W Z_{11}), \quad (12)$$

where Z_{1j} describe the field content of the LSP [94]. Clearly for the Higgs exchange to contribute requires a LSP with some Higgsino component ($Z_{13}, Z_{14} \neq 0$) In all models where Higgs exchange dominates we expect $\lambda_p = \lambda_n$ within a 2% accuracy. This is because the quark coefficients in protons and neutrons are the same for heavy quarks and the largest coefficient is the one for squark.

For the spin-dependent amplitude, the Z exchange contribution reads,

$$\xi_N = -\frac{1}{2}(\Delta_u^N - \Delta_d^N - \Delta_s^N) \frac{g^2}{4M_Z^2 c_W^2} (Z_{13}^2 - Z_{14}^2). \quad (13)$$

When the squark contribution is negligible the ratio of proton to neutron amplitudes ξ_p/ξ_n is therefore totally independent of the neutralino coupling to the Z. We expect $\tan\phi = \xi_p/\xi_n \approx -1.14 \pm 0.03$ when considering the range for the quark coefficients specified in Eq. (6). This value for $\tan\phi$ is expected in any model where Z exchange dominates the spin-dependent interaction.

These simple relations are spoiled in models where squarks are light unless squarks of different flavors are nearly degenerate in which case we still expect $\lambda_p/\lambda_n \approx 1$. Strong corrections to this ratio can be found when $m_{\tilde{q}_{L,R}} \approx m_\chi$ since in this case twist-2 operators give a large contribution that can even cancel the leading s-quark contribution [84]. Note that a twist-2 contribution, being proportional to the quark hypercharge, is larger for u-squarks so it will contribute mainly to the proton amplitude. In principle, the impact of light squarks is more important for spin-dependent interactions because of a possible cancellation between u- and d-type quark coefficients. However, the squark exchange is dominant for SD cross sections that are usually too small to be measured even in ton-scale detectors.

The ratio of SD to SI amplitudes also characterizes the model. When sfermions are heavy, the relic density of dark matter favors a LSP with some wino or Higgsino component. In such models the ratio of spin-dependent to spin-independent interactions depends strongly on the Higgsino component of the LSP, Eqs. (11) and (13), and predictions can vary in a wide range.

B. Right-handed neutrino model (RHNM)

A model with warped extra dimensions where the CDM is a right-handed Dirac neutrino was proposed by Agashe and Servant [95]. This model contains both new fermions and new gauge bosons at the (multi-)TeV scale which interact mainly with third generation fermions. This model can be used as a prototype of a more general class of

models with a right-handed Dirac neutrino as CDM [96]. Whether or not there are additional quarks or gauge bosons, because of the large mass scale involved, the most important contribution to elastic scattering of the right-handed neutrino on nucleons is due to Z and Higgs exchange [95]. What is peculiar in this class of models is that the CDM is not a Majorana particle, so there is an important contribution of Z exchange to both SI and SD nucleon scattering [84]. Typically in this model the elastic scattering cross sections are large and direct detection poses one of the strongest phenomenological constraint on the model [96].

For the dominant Z exchange contribution to the spin-independent interactions

$$\lambda_p = \frac{g_Z^{\nu_R} e(1-4s_W^2)}{8M_Z^2 s_W c_W} \quad \text{and} \quad \lambda_n = \frac{g_Z^{\nu_R} e}{8M_Z^2 s_W c_W}, \tag{14}$$

where $g_Z^{\nu_R}$ is the parameter that describes the coupling of ν_R to the Z. This coupling is induced through mixing so is suppressed with respect to the SM couplings. The neutron and proton amplitudes are directly related [95],

$$\frac{\lambda_p}{\lambda_n} = (1-4s_W^2) \approx 0.09 \tag{15}$$

for $s_W^2 = 0.228$. If the ν_R also couples to the Higgs, both λ_p and λ_n will receive the same additional contribution, thus modifying the simple relation, Eq. (15). In the numerical analysis we will include a generic coupling of the Higgs to the neutrino g_H [96].

For spin-dependent interactions which also proceed through Z exchange, we get

$$\xi_N = \sum_{q=u,d,s} b'_q \Delta_q^N \quad \text{where } b'_q = \frac{g_Z^{\nu_R}(g_R^q - g_L^q)}{4M_Z^2} \tag{16}$$

and $g_R^d - g_L^d = -(g_R^u - g_L^u) = \frac{e}{2s_W c_W}$. As for the MSSM, the ratio of proton to neutron amplitudes, $\tan\phi = \xi_p/\xi_n = -1.14 \pm 0.03$.

In the limit that the Higgs contribution is negligible, the ratio of SD to SI amplitudes is also independent of the details of the model with $\xi/\lambda_+ = 1.06 \pm 0.02$ when varying the quark coefficients in the range specified in Eq. (6).

C. Minimal universal extra-dimensions model (MUED)

In the universal extra-dimensions model (UED) potential dark matter candidates include a KK gauge boson, a KK neutrino, a KK scalar, or a KK graviton [10,37,97]. We restrict our analysis to the minimal UED model (MUED), in which case the CDM is either the first KK level of the hypercharge gauge boson, B^1, or the KK graviton. We will consider only the former possibility since the graviton has small direct detection rates. CDM scattering on nucleon proceeds both through Higgs exchange and KK-quark exchange. For spin-independent interactions, the nucleon amplitude reads [19]

$$\lambda_N = \frac{m_N}{8m_{B_1}} \sum_q \left(\frac{g_1^2}{m_h^2} + 2g_1^2(Y_{q_L}^2 + Y_{q_R}^2) \frac{M_{B_1}^2 + M_{q^1}^2}{(M_{B^1}^2 - M_{q^1}^2)^2} \right) f_q^N, \tag{17}$$

where the sum is over all quark flavors and $g_1 = e/c_W$, $Y_{q_L} = 1/6$, $Y_{u_R} = -2/6$. The first term arises from Higgs interactions and the second term from KK quarks exchange. In this model it is quite natural to have a large contribution from KK quarks since they are nearly degenerate with the CDM. We include radiative corrections to level 1 KK states [18] which lead to mass splittings between KK quarks and B^1. Note that the Higgs contribution is suppressed compared to the MSSM by a factor m_W/m_{B_1} as well as by the Higgs mass which is usually larger than in the MSSM. Nevertheless one expects $\lambda_p/\lambda_n \approx 1$ as in models where the Higgs exchange dominates because all new quarks are nearly degenerate.

For spin-dependent interactions, the amplitude reads

$$\xi_N = \frac{1}{\sqrt{6}} \sum_{q=u,d,s} 2g_1^2(Y_{q_L}^2 + Y_{q_R}^2) \frac{1}{(M_{q^1}^2 - M_{B^1}^2)} \Delta_q^N \tag{18}$$

and is solely due to KK-quarks exchange. One can easily show that $\tan\phi = \xi_p/\xi_n \approx -3.5$ independently of the parameters of the model as long as all KK quarks are degenerate. The ratio ξ/λ_+ can be large and is controlled by the B_1 mass and by the mass splitting with the KK quarks when these dominate the SI interaction.

D. Little Higgs model (LHM)

In the little Higgs model with T-parity, the dark matter candidate is the lightest new heavy neutral gauge boson A_H [98,99]. This model therefore shares many aspects of the MUED model just discussed, the CDM is a gauge boson, spin-independent interactions are due to Higgs and heavy quark exchange, while only the latter contributes to spin-dependent interactions. The expressions for both SI and SD amplitudes are the same as above, Eqs. (17) and (18). There are however two important differences between these models: first the hypercharges of the heavy quarks are small, $Y_{q_L} = 1/10$, $Y_{q_R} = 0$. Second, the mass splitting between the new heavy quarks Q and A_H is typically much larger than in the MUED model, which means that the heavy quark contribution to DD is suppressed. One therefore expects an overall low rate $\sigma_{\chi N}^{\rm SI}$ and $\lambda_p/\lambda_n \approx 1$ when Higgs exchange dominates or heavy quarks are nearly degenerate. Because there is no Z exchange diagram the SD interaction should also be much suppressed unless one artificially requires a small mass splitting between the heavy photon and heavy quarks, Eq. (18). It is only in this case that one expects to have a detectable cross section. Then $|\phi|$ will depend strongly on the mass difference between the heavy photon and the lightest new quark and should be large.

E. Scalar dark matter

Simple models with an additional scalar field that is basically decoupled from the SM sector have been proposed [22–24]. In these models, the CDM candidate is a new scalar field. We consider the inert doublet model (IDM) [23], a two Higgs doublets extension of the standard model with a Z_2 symmetry. One of the two doublets and the usual standard model particles are even under this symmetry. The new particles of the model are a neutral (H^0), a pseudo (A), and a charged (H^+) scalar. Depending on the parameters of the model, the dark matter candidate can be H^0 or A. Only spin-independent interactions can occur through either $H^0 q \to {}^h H^0 q$ and $H^0 q \to {}^Z A q$. The latter has to be kinematically forbidden, that is $M_A - M_{H^0} > 100$ keV, to respect the current experimental constraints. The h exchange cross section driven by an effective coupling λ_L [23] is

$$\sigma_{\chi N} = \frac{\mu_\chi^2}{4\pi}\left(\frac{\lambda_L}{M_{H_0} M_h^2}\right)^2 \left(\sum_q f_q^N\right)^2 m_N^2, \tag{19}$$

where $\chi = H^0$.

IV. RESULTS

Here we present numerical results for each of our sample models. Amplitudes and cross sections for direct detection are computed with micrOMEGAs2.2 and in each case include all tree-level diagrams, the contribution of twist-2 operators as well as QCD corrections. Additional SUSY-QCD corrections are included in the MSSM as discussed in [84]. The computation of the CDM relic density is also based on micrOMEGAs2.2 [100,101]. We fix $m_t = 172.6$ GeV. We also restrict the parameter space to a CDM particle roughly below the TeV scale simply because detectors are not as sensitive to heavier CDM particles. We also never consider $m_h > 500$ GeV, although allowed in some models such a Higgs gives a small contribution to direct detection.

We first summarize for each model the predictions for both $\sigma_{\chi N}^{\rm SI}$ and $\sigma_{\chi N}^{\rm SD}$. We always impose the upper limit from the relic density of dark matter $\Omega h^2 < 0.136$ [102] in our scans as well as other model dependent constraints on the parameters of each model. When specified we also impose the lower bound $\Omega h^2 > 0.094$ [102]. We then compare the ratio of amplitudes on neutrons and protons $(\phi, \xi/\lambda_+, \lambda_p/\lambda_n)$ before comparing the rates on various nuclei. We have taken into account the theoretical uncertainty in the coefficients that relate the amplitude for quarks to the one in nucleons by varying the input parameters in the range specified in Eqs. (3) and (6).

A. Predictions for $\sigma_{\chi N}^{\rm SI}$ and $\sigma_{\chi N}^{\rm SD}$

1. MSSM

We consider two specific classes of the generic MSSM, as mentioned above. In the first class, MSSMH, squarks are heavy and we assume only universality among two of the gaugino masses at the GUT scale, that is $M_3 = 3M_2$ at the weak scale. In the second class, MSSMQ, we allow for light squarks, for simplicity we also impose full universality of the gaugino masses, which leads at the weak scale to $M_3 = 3M_2 = 6M_1$. In all cases we assume heavy sleptons.

For each model we have scanned over 10^5 scenarios varying the model parameters defined at the weak scale in the range

$$\begin{aligned} &100\ \text{GeV} < M_1 < 1000\ \text{GeV};\\ &100\ \text{GeV} < \mu < 2000\ \text{GeV}\\ &100\ \text{GeV} < m_A < 2000\ \text{GeV};\\ &2 < \tan\beta < 52 \end{aligned} \tag{20}$$

and

$$\begin{aligned} &\text{MSSMH}: 100\ \text{GeV} < M_2 < 1000\ \text{GeV};\\ &M_{\tilde{q}_{L,R}} = 2\ \text{TeV} \qquad \text{MSSMQ}: M_2 = 2M_1;\\ &M_{\tilde{q}_{L(R)}} < 2M_\chi; \qquad M_{\tilde{q}_{R(L)}} = 2\ \text{TeV}. \end{aligned} \tag{21}$$

For this range of parameters the mass of the DM particle does not exceed 1 TeV. In each case the LEP limits on Higgs and SUSY particles are imposed as well as the upper bound on the CDM relic density.

The predictions for the SI and SD cross sections in MSSMH are displayed in Fig. 1(a) together with the reach of future ton-scale detectors. The absolute bound for CDMS/Xenon is indicated only to guide the eye as this limit depends on the CDM mass. Virtually all scenarios will be accessible to future searches for SI interactions. This is a direct consequence of imposing the constraint from the relic density which requires a neutralino DM with some Higgsino component for efficient annihilation. This then automatically leads to a χ_1^0 coupling to the light Higgs hence to a non-negligible cross section for SI elastic scattering. The smallest cross sections in Fig. 1(a) correspond to a neutralino with a very small Higgsino fraction that nevertheless annihilate efficiently because it does so near a heavy Higgs resonance. Models with a relic density within the Wilkinson Microwave Anisotropy Probe (WMAP) range (rather than only below the upper bound) almost span the full range of predictions for SI and SD cross sections, although many of the scenarios with the largest $\sigma_{\chi N}^{\rm SI}$ have a large Higgsino component and are associated with a small value for the relic density due to the efficient annihilation into W pairs. The Higgsino component also induces a coupling to the Z hence leads to SD interactions. Because these interactions are not coherent in several cases the predictions can be as low as $\sigma_{\chi p}^{\rm SD} \approx 10^{-9}$ pb, much

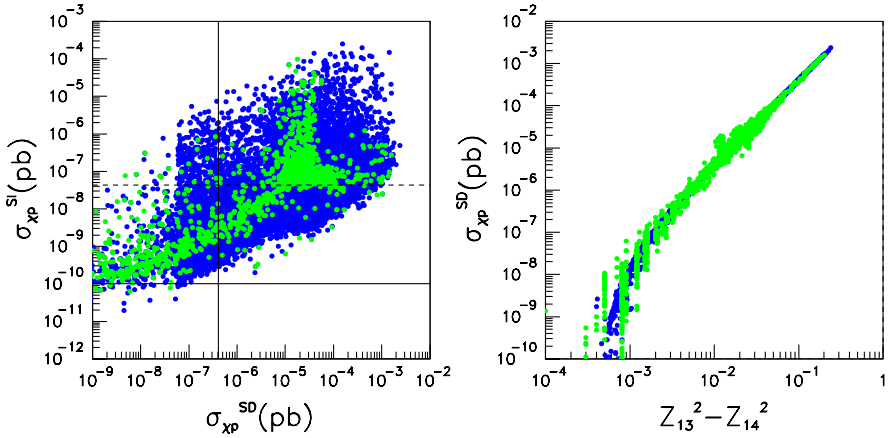

FIG. 1 (color online). (a) Predictions for $\sigma_{\chi p}^{\mathrm{SI}}$ vs $\sigma_{\chi p}^{\mathrm{SD}}$ in MSSMH. In blue the scenarios that satisfy the WMAP upper bound and in green those that have $0.094 < \Omega h^2 < 0.136$. For easy reference the present absolute lower limit from CDMS/Xenon is indicated (dash) as well as future limits from large scale detectors (full) (b) $\sigma_{\chi p}^{\mathrm{SD}}$ as a function of $Z_{13}^2 - Z_{14}^2$ in MSSMH.

below the expected reach of future detectors. Note that because Z exchange dominates SD interactions, the rate is directly related to the $Z\chi\chi$ coupling which is proportional to $Z_{13}^2 - Z_{14}^2$, Eq. (13). A rate measurement will therefore set a limit on this coupling assuming the MSSMH, see Fig. 1(b).

In MSSMQ, the range of predictions for $\sigma_{\chi p}^{\mathrm{SI}}$ is roughly the same as in MSSMH, see Fig. 2(a) although cross sections below the reach of future SI detectors can be expected in a few cases. Furthermore, large cross sections for SD interactions can be expected even when SI ones are quite low. In general this occurs in scenarios with light squarks. There is no explicit correlation between $\sigma_{\chi N}^{\mathrm{SI}}$ and the mass of the CDM, see Fig. 1(b), although models with a neutralino around 60 GeV that annihilate near a light Higgs resonance can have small cross sections. We explicitly display in Fig. 3(b), the CDMS exclusion limit for both MSSMH and MSSMQ. Many scenarios are excluded even when taking into account a large uncertainty (up to a factor 3 [85]) in the exclusion limit that could arise from the DM distribution.

2. RHNM

In the right-handed neutrino model we use as free parameters the mass of the CDM, its coupling to the Z, $g_Z^{\nu_R}$, and to the Higgs, g_H, as well as the mass of the Higgs. We assume all other particles in the model to be above 3 TeV and therefore do not play a role in direct detection. We perform a scan over 100 000 models varying the free parameters in the range

$$30\ \mathrm{GeV} < m_{\nu_R} < 1200\ \mathrm{GeV}; \quad 120\ \mathrm{GeV} < m_h < 500\ \mathrm{GeV}$$
$$0.001 < g_Z^{\nu_R} < 0.01; \quad 0.01 < g_H < 0.25. \tag{22}$$

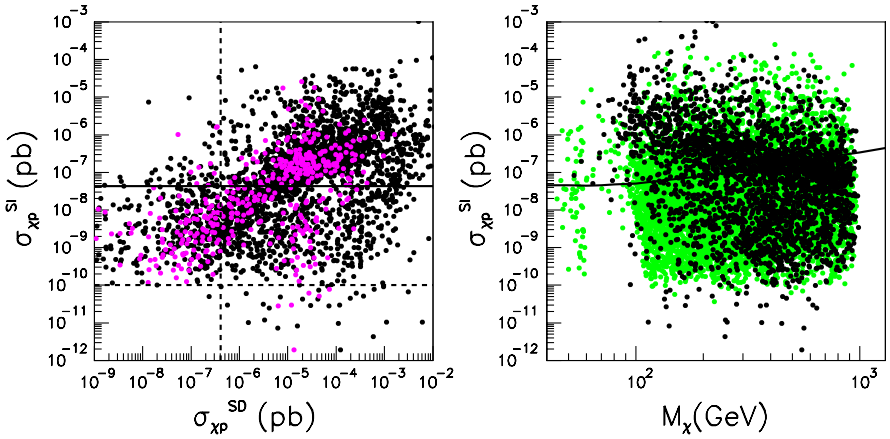

FIG. 2 (color online). (a) Predictions for $\sigma_{\chi p}^{\mathrm{SI}}$ vs $\sigma_{\chi p}^{\mathrm{SD}}$ in MSSMQ. In black the scenarios that satisfy the WMAP upper bound and in green those that have $0.094 < \Omega h^2 < 0.136$. For easy reference the present absolute lower limit from CDMS/Xenon is indicated (full) as well as future limits from large scale detectors (dash) (b) $\sigma_{\chi p}^{\mathrm{SI}}$ as a function of the neutralino mass in MSSMQ (black) and MSSMH (green).

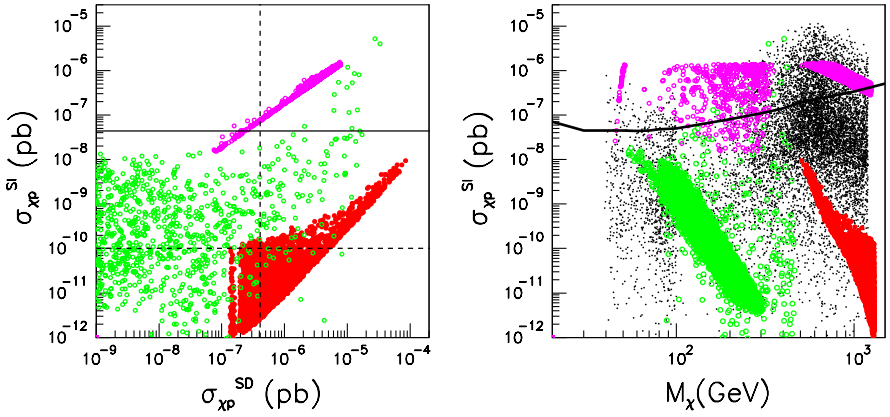

FIG. 3 (color online). Predictions for $\sigma^{\rm SI}_{\chi p}$ vs $\sigma^{\rm SD}_{\chi p}$ in MSSMQ (black), MUED (red), LHM (green), RHNM (pink). (b) $\sigma^{\rm SI}_{\chi p}$ as a function of the CDM mass, same color code as (a) with in addition the model IDM (black).

The range of $g_Z^{\nu_R}$ is chosen so that the upper bound on Ωh^2 is easily satisfied while not giving too large $\sigma^{\rm SI}_{\chi N}$ whereas the range for the Higgs coupling g_H is set so that the Higgs can potentially play a role in DD. Models with a Dirac right-handed neutrino often have an extended gauge sector. Since this is mostly relevant for the annihilation of a CDM particle beyond the TeV scale, we can safely ignore this sector in our analysis.

In this model one expects rather large rates for SI interactions, and this is in fact the most severe constraint on the model. Furthermore, a strong correlation is expected between the SI and SD rates as seen in Fig. 3(a). Indeed these rates are governed by the standard model axial and axial-vector $Z\bar{q}q$ couplings. Note that the limit extracted from $\sigma^{\rm SI}_{\chi N}$ has to be rescaled to take into account the fact that in this model $\lambda_p \ll \lambda_n$. In practice it means rescaling the limit by a factor 2–3 depending on the material. Even taking this factor into account Fig. 3(a) shows that models that will not be excluded in the near future predict a low rate for $\sigma^{\rm SD}_{\chi p}$. The mass of the CDM allowed in this model is either near $M_Z/2$, $M_H/2$ or above 500 GeV [96].

3. MUED

For the computation of the direct detection rate in the MUED model we include the level one KK quarks as well as the lightest Higgs exchange. We ignore the level 2 Higgs since in elastic scattering cross sections a heavy Higgs suffers from a mass suppression. Furthermore, the coupling of the level 2 Higgs to the B^1 is loop induced hence suppressed. Note, however, that because $M_{H^2} \approx 2M_\chi$ the level 2 Higgs plays a role in the computation of the relic density [103,104]. The impact of neglecting this coupling on our analysis is not significant as the majority of the models already has $\Omega h^2 < 0.136$.

The free parameters of the model are $1/R$, the inverse size of the extra dimension that determines the mass of the KK states, Λ, the cutoff scale, and m_h the lightest Higgs mass. We scan over 10^5 scenarios with the three free parameters of the model in the following range

$$300\ \text{GeV} < 1/R < 1300\ \text{GeV}; \qquad 3 < \Lambda R < 50; \qquad 120\ \text{GeV} < m_h < 500\ \text{GeV}. \tag{23}$$

The precision electroweak constraints set the lower bound on $1/R$ [105] while perturbativity and unitarity constraints set a range for ΛR [106]. The mass of all KK states are computed including one-loop corrections [107]. The radiative corrections will induce a small mass splitting between the level one B^1 boson and KK fermions. Such splitting is typically 1%–2% for KK-leptons and 5%–25% for KK quarks and strongly influences the direct detection rate. We also ensure that the CDM relic density satisfies the WMAP upper bound and that the charged Higgs is not the CDM.

The SI cross sections are suppressed by the heavy B_1 mass, Eq. (17), the larger cross sections are therefore expected for the lighter CDM particles, see Fig. 3(b). Typically, more than an order of magnitude improvement in detectors sensitivities is needed to probe the parameter space of the model and a large fraction of the models, specially those with a CDM at the TeV scale, will remain inaccessible to the large scale detectors. The main characteristic of this model is the correlation between SI and SD cross sections, this is because the heavy KK-quark exchange contributes to both modes. As a result, SD interactions could be accessible in cases where rates are too low for SI interactions. This is in sharp contrast with the MSSMH.

4. LHM

The LHM with T-parity contains in addition to heavy gauge bosons, heavy T-odd fermions as well as a new T-even heavy top quark. We choose as free parameters the Higgs mass, f, κ and s_α. f sets the scale of the heavy gauge bosons and fermions, in particular, the heavy photon of mass

$$M_{A_H} = \frac{g' f}{\sqrt{5}}\left[1 - \frac{5v^2}{8f^2}\right] \tag{24}$$

with v the usual vev of the Higgs. κ is an additional parameter that enters the fermion masses, for example, for a heavy down-type quark, $M_d = \sqrt{2}\kappa f$. For simplicity we assume an universal factor κ for all heavy fermions. s_α depends on the ratio of the Yukawa couplings of T-even and T-odd top quarks. [108] This parameter enters the top quark mass as well as couplings involving standard and heavy top quarks.

We scan over 10^5 scenarii varying randomly the free parameters in the range

$$500\ \text{GeV} < f < 3000\ \text{GeV}; \qquad 120\ \text{GeV} < m_h < 500\ \text{GeV}$$
$$0.1 < s_\alpha < 0.96; \qquad 0.11 < \kappa < 1. \tag{25}$$

We impose the LEP limits on the production of heavy quarks as well as on the Higgs mass.

The rates for both SI and SD cross sections are in general quite low, even below the scale in Fig. 3(a). As we have explained before, this is due to the small hypercharge of the heavy quarks as well as to their generally large mass. Models that could lead to a signal in either the SI or SD channel are those where the mass splitting between heavy quarks and the heavy photon is between 1%–10% or slightly larger if the heavy quarks are around 100 GeV. Furthermore, the heavy photon has to be rather light with $M_{A_H} < 400$ GeV, see Fig. 3(b). A Higgs near the lower LEP limit also helps increase the signal for SI interactions. Note that since it is the new quarks that couple to the nucleon that need to be light, mainly the first and second generation, the recent Tevatron limit on the heavy top quark [109] does not play a role here.

5. IDM

In the IDM, the free parameters are those of the Higgs potential [23]. We choose to use rather the physical parameters, the masses of the CDM candidate, m_{H^0}, the light scalar, m_h, the pseudoscalar, m_A, and the charged Higgs, m_{H^+} as well as two parameters of the Higgs potential μ_2 and λ_2. Our numerical results are not very sensitive to the value of λ_2 so for simplicity we fix $\lambda_2 = 0.1$. Other free parameters are varied in the range

$$10\ \text{GeV} < m_{H^0} < 1200\ \text{GeV};$$
$$115\ \text{GeV} < m_h < 500\ \text{GeV}; \tag{26}$$
$$10\ \text{GeV} < \mu_2 < 1200\ \text{GeV}$$

with in addition the following range for the mass differences

$$5\ \text{GeV} < m_A - m_{H^0} < 15\ \text{GeV};$$
$$40\ \text{GeV} < m_{H^+} - m_{H^0} < 50\ \text{GeV} \tag{27}$$

if m_{H^0}, $\mu_2 < 100$ GeV, otherwise

$$3\ \text{GeV} < m_A - m_{H^0} < 6\ \text{GeV};$$
$$5\ \text{GeV} < m_{H^+} - m_{H^0} < 10\ \text{GeV}. \tag{28}$$

We impose the following constraints on the model: vacuum stability and perturbativity conditions on the potential parameters, LEP limit on the charged Higgs, contribution to the Z boson width, and electroweak precision constraints [45].

The rates for $\sigma^{\text{SI}}_{\chi N}$ varies over several orders of magnitude and the masses of the CDM particle ranges anywhere from 50 GeV to the TeV scale, Fig. 3(b). Note, however, that once one imposes a lower bound on Ωh^2, the ranges for the masses and the direct rates are severely restricted, see Sec. IV D.

B. Discriminating models: Amplitudes for scattering on protons and neutrons

The ratios of proton to neutron amplitudes apart from being free of large theoretical uncertainties provide a good model discriminator. For this to be useful, one has to assume that these quantities can be measured; this means that in this section we keep only models for which $\sigma^{\text{SI}}_{\chi N} > 10^{-10}$ pb and $\sigma^{\text{SD}}_{\chi N} > 4. \times 10^{-7}$ pb. The more challenging case with only a detectable SI cross section will be discussed in the subsection IV D.

The results of the parameter scan for the five models under consideration are displayed in Fig. 4(a)–4(c) for $\phi = \arctan(\xi_p/\xi_n)$ vs ξ, ξ/λ_+ and λ_p/λ_n. The ratio of SD neutron to proton amplitudes, $\tan\phi$, can discriminate models where the SD interaction is dominated by Z exchange (MSSMH and RHNM) from those where it is dominated by (s)quark exchange (LHM, MSSMQ, and MUED). The ratio of SD/SI amplitudes, ξ/λ_+ which can be much larger in the MUED or in the MSSM could provide further discrimination. The parameter λ_p/λ_n can in principle disentangle further some models where the SI interaction is dominated by H exchange or by Z exchange (RHNM), see Fig. 4(c). Unfortunately in practice different materials are not very sensitive to this quantity. Note also that the effect of twist-2 operator in MSSMQ and LHM can be important and lead to large corrections to the expected value of $\lambda_p/\lambda_n \approx 1$.

The mass determination in the DD experiment from the shape of the energy spectrum could in some cases provide additional information to discriminate between models. In particular one could distinguish the LHM, which allows a CDM in the range $M_{A_H} \approx 50$–120 GeV from MUED which requires a heavy CDM particle and even sometimes from the MSSMQ, which predicts a large range for the masses Fig. 4(d). The LHC, with its potential for discovery of colored particles, will establish whether or not colored particles could play a role in direct detection. Indeed in all LHM predicting a signal in DD or in the MSSMQ models,

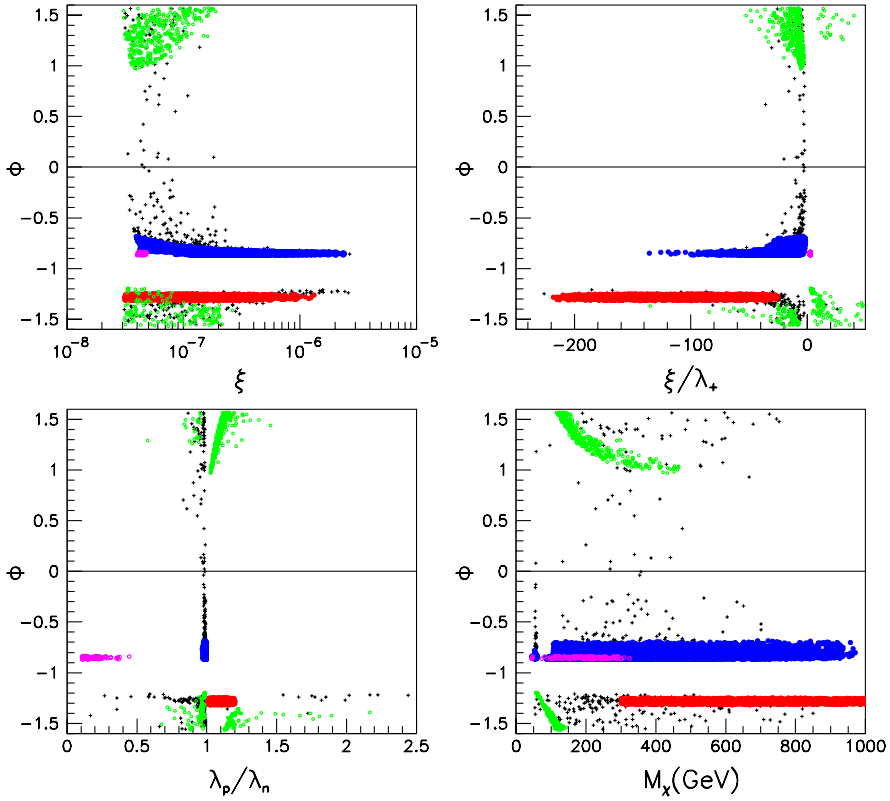

FIG. 4 (color online). Predictions for (a) $\phi = \text{atan}(\xi_p/\xi_n)$ as a function of ξ (b) ξ/λ_+ (c) λ_p/λ_n (d) M_χ in models MSSMH (blue), MSSMQ (black), MUED (red), LHM (green), and RHNM (pink). Only models for which $\sigma^{\text{SI}}_{\chi p} > 1.0 \times 10^{-10}$ pb and $\sigma^{\text{SD}}_{\chi p}$ or $\sigma^{\text{SD}}_{\chi n} > 4.0 \times 10^{-7}$ pb are included.

the heavy quarks and squarks can be produced easily as they lie well below 2 TeV. The heavy quarks can be just beyond the LEP exclusion bound, $M_{Q_H} = 100$–400 GeV in the LHM while in the MSSMQ models that have a large value for $|\phi|$ squarks can be as heavy as $M_{\tilde{q}} < 900$ GeV. The heavier squarks occur when the neutralino has a large Higgsino content. We will not pursue a detailed analysis of what can be measured at the LHC, this is beyond the scope of this paper. We note, however, that the mass splitting is an issue regarding the LHC potential for discovering new colored particles, for small mass splitting the signals for the new particles will be hard to extract from the background. This could be crucial for the LHM where the mass splitting between the CDM and the heavy quark is below 10%. In the MUED model the mass splitting is between 6%–22% and has been shown to be sufficient for providing a signal in four leptons + missing energy channel [46]. In MSSMQ the mass splitting is also typically around 20%. To completely discriminate between the models at the LHC would, however, also require spins of the new colored particles to be measured [110].

C. Direct detection rates on nuclei

Having established that a combined measurement of the amplitudes for SI and SD interactions on protons and neutrons can in principle distinguish between the underlying particle physics models, up to a few ambiguities, we now compare various models' predictions for quantities that are closely related to the observables. As before, we only include scenarios that could eventually lead to a signal in a large detector in both the SI and SD modes. We consider a selection of nuclei that are currently used in large detectors. Those include the nuclei sensitive only to SI interactions such as ^{40}Ar, ^{76}Ge as well as nuclei with an odd nucleon that are also sensitive to SD interactions on either protons, ^{19}F, ^{23}Na, ^{127}I, ^{133}Cs or neutrons ^{29}Si, ^{73}Ge, ^{129}Xe, ^{131}Xe. For each nucleus N we compute the total event rate, $n(N)$ for a recoil energy above 2 keV. For heavy nuclei, say ^{129}Xe, the rate is correlated with the value of λ_+ while for light nuclei like ^{19}F the correlation is spoiled by the SD contribution. This is illustrated in Fig. 5 for both MUED and MSSMQ. The total number of events varies over several order of magnitude for these two models. The rates are generally expected to be larger for heavy nuclei, especially in models with a suppressed SD contribution like RHNM. In this model the total number of events in n(F) varies between $0.4 - 4.0 \times 10^{-3}$ (events/kg/day).

To eliminate as much as possible the astrophysical and nucleon ambiguities we compare ratios of rates for scattering on different nuclei. We define the ratios $R_{N_1/N_2} = n(N_1)/n(N_2)$. We first compute the ratios R_{N_1/N_2} for SD

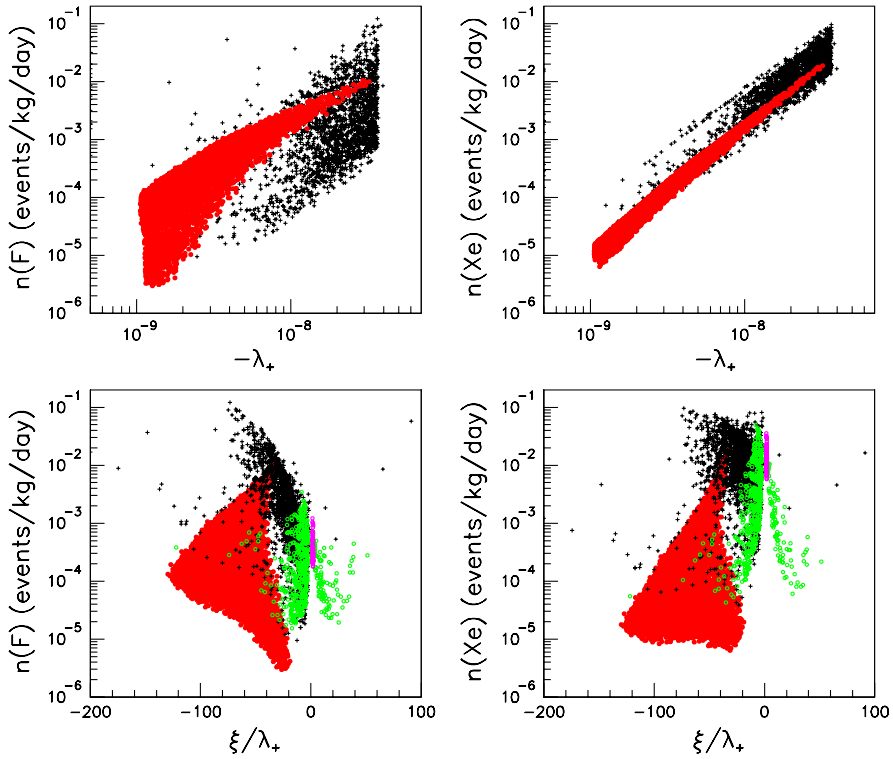

FIG. 5 (color online). Total rates (events/kg/day) (a) n(F) and (b) n(Xe) vs λ_+ (c) n(F) and (d) n(Xe) vs ξ/λ_+ in models MSSMQ (black) and MUED (red). Predictions for rates in LHM (green) and RHNM (pink) are also included in (c)–(d). Only models for which $\sigma^{\mathrm{SI}} > 1.0 \times 10^{-10}$ pb and $\sigma^{\mathrm{SD}} > 4.0 \times 10^{-7}$ pb are included.

proton sensitive over SD neutron sensitive nuclei in our sample models. Such ratios are expected to feature a dependence on $\tan\phi = \xi_p/\xi_n$ as well as on ξ/λ_+ when a heavy nucleus is involved.

The results of a scan over the parameter space of each of our sample models are displayed in Fig. 6(a). The comparison of $R_{\mathrm{F/Xe}}$[4] and $R_{\mathrm{I/Si}}$ provides a good model discriminator with, in particular, only a small overlap between the predictions of MSSMH and MUED. This is a direct consequence of the large value for $\tan\phi$ and ξ in MUED. In this model, ^{127}I is very sensitive to SD interactions since ξ_p is enhanced, thus $R_{\mathrm{I/Si}}$ is determined by the SD interaction and is large. On the other hand in MSSMH, ^{127}I is mostly sensitive to SI interactions thus $R_{\mathrm{I/Si}}$ can be reduced significantly in the scenarios where ξ is large. Recall that those are the scenarios with a large Higgsino fraction. Such scenarios are precisely those that lead to a value for $R_{\mathrm{F/Xe}}\tilde{\mathcal{O}}(1)$ and that could have been confused with MUED. Indeed in MUED most scenarios predict $R_{\mathrm{F/Xe}} > 1$ because of an important SD amplitude. The LHM and MSSMQ scenarios that predict large values for $\tan\phi$, those with a (s)quark that is almost degenerate with the CDM particle have predictions similar to MUED for both ratios. Note that in the MSSMQ when the squark contribution is important, there can be a partial cancellation between the various quarks contributions in the neutron amplitudes such that $\xi_n \ll \xi_p$ ($\phi \approx -\pi/2$). Then n(F) and to a lesser extent n(I) are enhanced but not n(Si), these scenarios correspond to the few points in Fig. 6(a) with large R(F/Xe) and large R(I/Si). ^{23}Na is another light nuclei that shares most of the characteristics of F albeit with a reduced sensitivity to the SD part, see Fig. 6(c) while ^{73}Ge is a heavy nuclei that share many of the features of Xe. The ratio $R_{\mathrm{F}/^{73}\mathrm{Ge}}$ spans roughly the same range than $R_{\mathrm{F/Xe}}$ in each model, see Fig. 6(b). The ratio $R_{\mathrm{I}/^{73}\mathrm{Ge}}$ just as $R_{\mathrm{I/Xe}}$ does not vary much in either MSSM or LHM, except in the special scenarios with much enhanced ξ_n. In MUED, $R_{\mathrm{I}/^{73}\mathrm{Ge}}$ goes from 1.5–3.5 with high values associated with large ξ/λ_+, see Fig. 6(d).

We also considered other combinations of nuclei including those that are primarily sensitive to spin-independent interactions. We found that the rates for $R_{^{76}\mathrm{Ge/Xe}}$, $R_{\mathrm{Ar/Xe}}$, $R_{\mathrm{Ar/Cs}}$, or $R_{\mathrm{Cs/Xe}}$ could also give a handle to discriminate models. The results of our scan of the parameter space in each of our sample models are displayed in Fig. 7 for a representative set of pairs of nuclei. As explained before, the rate in n(Xe) increases when ξ/λ_+ is large and the SD contribution important. This increase is driven by ξ_n so is more important in MSSMH than in MUED or LHM.

[4]For illustrative purposes we use ^{129}Xe in the figures, similar results are found for ^{131}Xe.

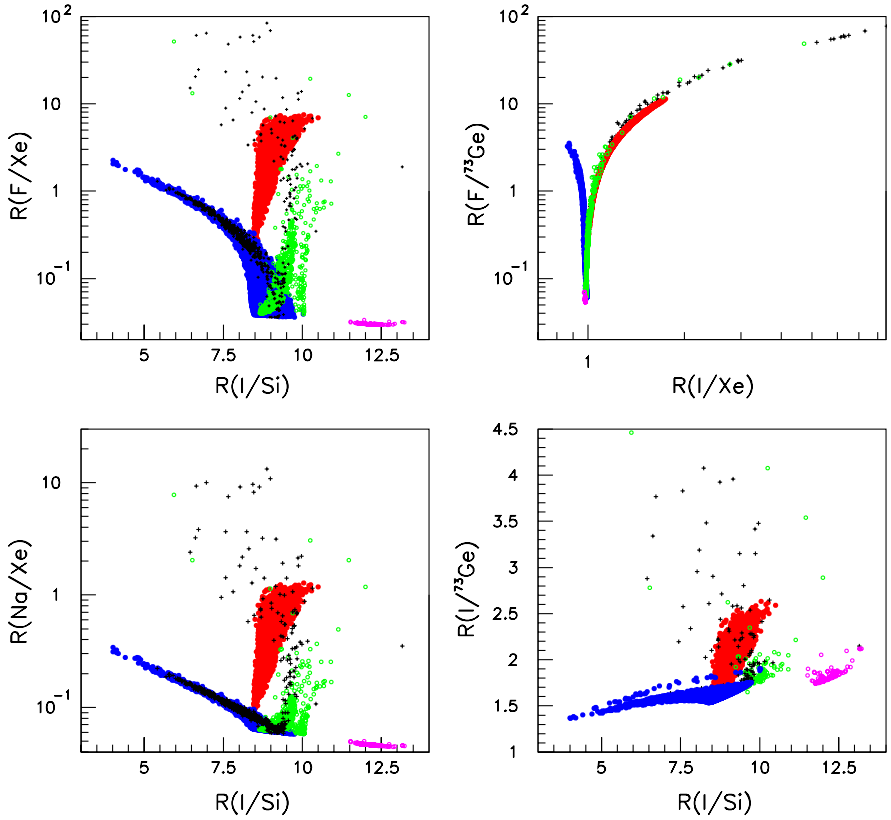

FIG. 6 (color online). Predictions for the ratio of total rates (a) $R_{\mathrm{F/Xe}}$ vs $R_{\mathrm{I/Si}}$, (b) $R_{\mathrm{F/Xe}}$ vs $R_{\mathrm{I/^{73}Ge}}$, (c) $R_{\mathrm{Na/Xe}}$ vs $R_{\mathrm{I/Si}}$, (d) $R_{\mathrm{I/^{73}Ge}}$ vs $R_{\mathrm{I/Si}}$ in different models, same color code as Fig. 4.

Therefore, reductions in the ratio $R_{^{76}\mathrm{Ge/Xe}}$ or $R_{\mathrm{Ar/Xe}}$ are larger in MSSMH than in other models, reaching almost a factor 2. On the other hand ^{133}Cs is sensitive to ξ_p thus the rate $n(\mathrm{Cs})$ can be large in MUED models leading to a suppression of $R_{\mathrm{Ar/Cs}}$ while for other models the predictions for $R_{\mathrm{Ar/Cs}}$ are very similar to those for $R_{\mathrm{Ar/Xe}}$. Note that in the MSSM, there are two disconnected regions in Fig. 7(a)–7(c). Although the difference is too small to be measured, the narrow band corresponds to models with a CDM around 50 GeV.

Heavy nuclei can also be used to identify models where $\tan\phi$ is large. Consider for example $R_{\mathrm{Cs/Xe}}$. Both nuclei have similar atomic number and are mainly sensitive to SI interactions, while ^{133}Cs is also sensitive to ξ_p and ^{129}Xe to ξ_n. In models where $\xi_p \gg \xi_n$, such as MUED and some of the MSSMQ and LHM scenarios, the ratio $R_{\mathrm{Cs/Xe}}$ can be as large as 2 while $R_{\mathrm{Cs/Xe}} \approx 1$ in all models where SI interactions dominate and/or $\xi_p \approx \xi_n$.

We conclude that in principle with the observation of signals in detectors with different materials, including detectors highly sensitive to SD interactions, discrimination of MUED from MSSMH and LHM is possible except in a small numbers of scenarios. On the other hand the model MSSMQ with light squarks can easily be confused with MUED and LHM. We do not attempt to estimate the precision to which the ratio of rates can be measured, it is strongly dependent on the specific detector in operation. A more precise analysis must await some signals.

D. SI interactions

The case where only a signal is observed in SI interactions has much less discriminating power. Basically the only information that can be used is the total cross section as well as the mass of the CDM particle. We have compared predictions for $\sigma^{\mathrm{SI}}_{\chi N}$ for all models considered previously including only scenarios where a signal would be seen only in the SI channel, that is $\sigma^{\mathrm{SI}}_{\chi N} > 10^{-10}$ pb and $\sigma^{\mathrm{SD}}_{\chi N} < 4 \times 10^{-7}$ pb. Here we include also the IDM which leads only to a signal in SI interactions. As discussed previously, the predictions for the RHNM are always large $\sigma^{\mathrm{SI}}_{\chi N} > 1.5 \times 10^{-7}$ pb and only a light CDM can be expected, see Fig. 8(a) while those of the LHM are much lower $10^{-8}\mathrm{pb} > \sigma^{\mathrm{SI}}_{\chi N} > 10^{-10}$ pb. In the MUED model, cross sections are very low and the CDM is in the TeV range making it very difficult to see a signal. In the IDM model the CDM is either expected to be around 50 GeV with cross sections that span over the full range while for heavier CDM particles the predictions do not exceed a few 10^{-9} pb. In the MSSM (only results for MSSMH are

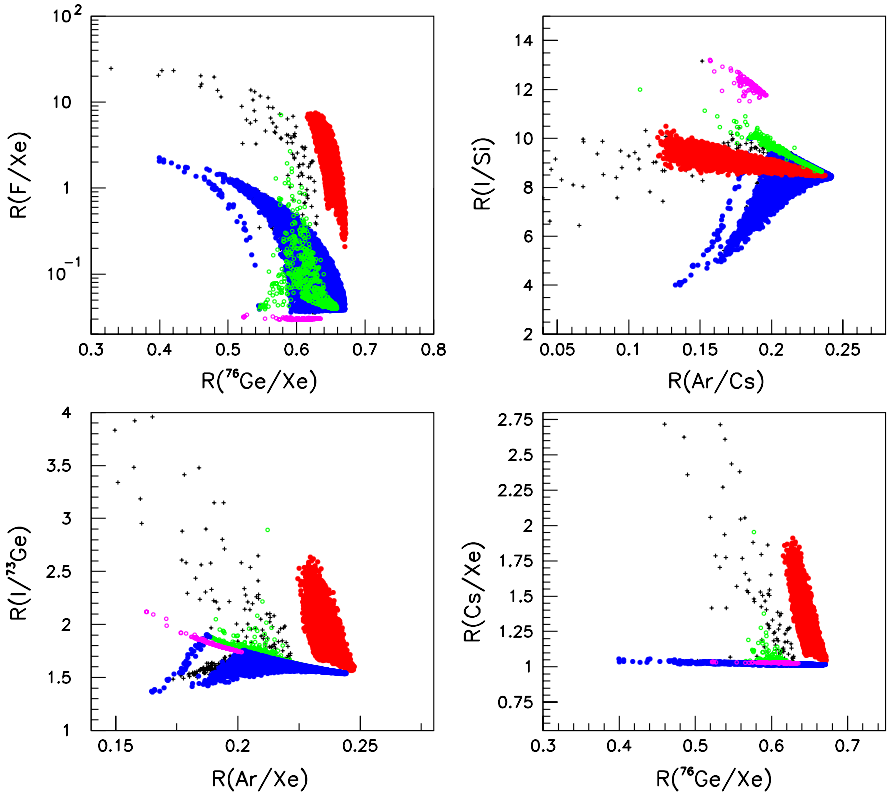

FIG. 7 (color online). Predictions for the ratio of total rates in (a) $R_{\mathrm{F/Xe}}$ vs $R_{^{76}\mathrm{Ge/Xe}}$, (b) $R_{\mathrm{I/Si}}$ vs $R_{^{76}\mathrm{Ge/Xe}}$, (c) $R_{\mathrm{I}/^{73}\mathrm{Ge}}$ vs $R_{\mathrm{Xe/Ar}}$, (d) $R_{\mathrm{Cs/Xe}}$ vs $R_{^{76}\mathrm{Ge/Xe}}$. Same color code as Fig. 4.

displayed in the figure, similar results are found for MSSMQ) the whole range of cross sections can be expected. For the IDM and MSSM we have imposed the WMAP lower and upper limit for the relic density. Allowing other dark matter candidates would lead to many more models passing the constraints and cross sections over the whole range for any CDM mass. To summarize, with only a signal in the SI channel one could distinguish RHNM from LHM, while IDM and MSSMH are often indistinguishable from each other and from the previous two models. A DM mass between 500–700 GeV is however only compatible with the MSSM. Furthermore, a heavier DM particle is only compatible with MSSM and IDM models while no signal is expected in the MUED model. These statements depend crucially on the upper bound that can be set on $\sigma^{\mathrm{SD}}_{\chi N}$. For example, if no signal is observed at the level of 10^{-5} pb we would predict that the SI cross section in MUED could reach $\sigma^{\mathrm{SI}}_{\chi N} \approx 10^{-9}$ pb, an order of magnitude more than what we have used in this section.

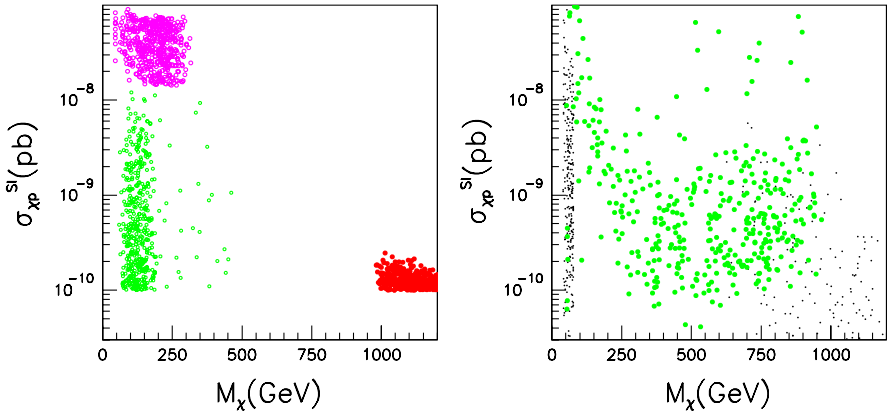

FIG. 8 (color online). Predictions for $\sigma^{\mathrm{SI}}_{\chi N}$ in scenarios where $\sigma^{\mathrm{SD}}_{\chi N} < 4. \times 10^{-7}$ pb (a) RHNM (pink), MUED (red), LHM (green) and (b) MSSMH (green) and IDM (black). In (b) only models that have $0.094 < \Omega h^2 < 0.136$ are included.

V. CONCLUSION

We have summarized the predictions for $\sigma^{\mathrm{SI}}_{\chi p}$ and $\sigma^{\mathrm{SD}}_{\chi p}$ in a variety of new physics models. We have emphasized the importance of measuring σ^{SD}_{N} to discriminate dark matter models although first signals are generally expected in the SI mode. This is because nuclei sensitive to SI interactions provide a measurement of basically one specific combination of couplings. On the other hand both amplitudes ξ_p and ξ_n can be measured with SD sensitive nuclei. Furthermore, most particle physics models predict $\lambda_p \approx \lambda_n$, at least those where the Higgs is responsible for SI interactions, while ξ_p/ξ_n vary over a very wide range, from $\xi_p/\xi_n \approx -1.1$ in models dominated by Z exchange to either very small or very large values when colored particles play an important role. To control astrophysical uncertainties as well as other theoretical uncertainties, we advocate to compare ratios of rates measured with different materials. These ratios can be powerful model discriminators especially when involving one light nuclei. In particular we have shown that in principle one could disentangle the MSSMH and MUED models. Recall that MSSMH is an example of a model with a Majorana neutralino where SI (SD) interactions are dominated by H(Z) exchange while MUED is a model where the same diagrams (quark exchange) contribute to both type of processes. Of course, the measurement of a total rate in SI interactions or better in SI and SD interactions will be sufficient to drastically reduce the parameter space of the various DM models and might even rule out some models, for example, the RHNM that requires a large rate for SI interactions. With direct detection alone it is much more difficult to distinguish MUED models from the LHM scenarios where the new quarks are almost degenerate with the CDM as well as with MSSM models with light squarks. This is because in this case the SI/SD amplitudes are also both dominated by the exchange of a colored particle. Fortunately, if these colored particles are below the 2 TeV scale, the LHC should be able to detect these new particles.

In this analysis we have considered all scenarios that could lead to a signal in large scale detectors, however in many scenarios signals are expected with the current generation of detectors. The results we have presented include those scenarios as well. There is, however, no guarantee that a positive signal will be measured for the full parameter space of the models we have considered. This is especially an issue for light nuclei. We have also shown explicitly that if the SD elastic scattering cross section is below the sensitivity of future detectors, it is much more difficult to identify the particle physics model with data from SI direct detection alone, The MSSM, LHM, and IDM models all predict $\sigma^{\mathrm{SI}}_{\chi p}$ in a wide range while a signal should be expected soon in the RHNM. In this case no signal is expected in MUED scenarios. A determination of the mass of the DM particle will help disentangle some models.

ACKNOWLEDGMENTS

We thank G. Azuelos, F. Boudjema, and V. Zacek for useful discussions. We thank A. Belyaev for providing the CalCHEP code for the little Higgs model. This work is supported in part by the GDRI-ACPP of CNRS and by the French ANR project ToolsDMColl, BLAN07-2-194882. The work of A. P. was supported by the Russian foundation for Basic Research, Grant No. RFBR-08-02-00856-a.

[1] D. N. Spergel *et al.*, Astrophys. J. Suppl. Ser. **170**, 377 (2007).
[2] M. Tegmark *et al.*, Phys. Rev. D **74**, 123507 (2006).
[3] J. R. Ellis, K. A. Olive, Y. Santoso, and V. C. Spanos, Phys. Lett. B **565**, 176 (2003).
[4] S. Profumo and C. E. Yaguna, Phys. Rev. D **70**, 095004 (2004).
[5] U. Chattopadhyay, A. Corsetti, and P. Nath, Phys. Rev. D **68**, 035005 (2003).
[6] H. Baer and C. Balazs, J. Cosmol. Astropart. Phys. 05 (2003) 006.
[7] D. Hooper and S. Profumo, Phys. Rep.**453**, 29 (2007).
[8] K. Kong and K. Matchev, J. High Energy Phys. 01 (2006) 038.
[9] F. Burnell and G. D. Kribs, Phys. Rev. D **73**, 015001 (2006).
[10] G. Servant and T. M. P. Tait, Nucl. Phys. **B650**, 391 (2003).
[11] G. Bertone, D. Hooper, and J. Silk, Phys. Rep. **405**, 279 (2005).
[12] H. Goldberg, Phys. Rev. Lett. **50**, 1419 (1983).
[13] J. R. Ellis, J. S. Hagelin, D. V. Nanopoulos, K. A. Olive, and M. Srednicki, Nucl. Phys. **B238**, 453 (1984).
[14] K. Agashe and G. Servant, Phys. Rev. Lett. **93**, 231805 (2004).
[15] K. Hsieh, R. N. Mohapatra, and S. Nasri, Phys. Rev. D **74**, 066004 (2006).
[16] T. Asaka, K. Ishiwata, and T. Moroi, Phys. Rev. D **75**, 065001 (2007).
[17] T. Appelquist, H.-C. Cheng, and B. A. Dobrescu, Phys. Rev. D **64**, 035002 (2001).
[18] H.-C. Cheng, K. T. Matchev, and M. Schmaltz, Phys. Rev. D **66**, 036005 (2002).
[19] G. Servant and T. M. P. Tait, New J. Phys. **4**, 99 (2002).
[20] J. Hubisz and P. Meade, Phys. Rev. D **71**, 035016 (2005).
[21] A. Birkedal, A. Noble, M. Perelstein, and A. Spray, Phys. Rev. D **74**, 035002 (2006).
[22] J. McDonald, Phys. Rev. D **50**, 3637 (1994).

[23] R. Barbieri, L. J. Hall, and V. S. Rychkov, Phys. Rev. D **74**, 015007 (2006).
[24] M. Lisanti and J. G. Wacker, arXiv:0704.2816.
[25] N. Arkani-Hamed, L. J. Hall, H. Murayama, D. Tucker-Smith, and N. Weiner, Phys. Rev. D **64**, 115011 (2001).
[26] H.-S. Lee, K. T. Matchev, and S. Nasri, Phys. Rev. D **76**, 041302 (2007).
[27] F. Deppisch and A. Pilaftsis, J. High Energy Phys. 10 (2008) 080.
[28] D. Majumdar, Phys. Rev. D **67**, 095010 (2003).
[29] D. G. Cerdeno, C. Munoz, and O. Seto, arXiv:0807.3029.
[30] V. Barger *et al.*, Phys. Rev. D **75**, 115002 (2007).
[31] D. G. Cerdeno, C. Hugonie, D. E. Lopez-Fogliani, C. Munoz, and A. M. Teixeira, J. High Energy Phys. 12 (2004) 048.
[32] A. Bottino, F. Donato, N. Fornengo, and S. Scopel, Phys. Rev. D**69**, 037302 (2004).
[33] A. Barrau *et al.*, Phys. Rev. D **72**, 063507 (2005).
[34] D. Hooper and G. D. Kribs, Phys. Rev. D **67**, 055003 (2003).
[35] G. Bertone, G. Servant, and G. Sigl, Phys. Rev. D **68**, 044008 (2003).
[36] L. Bergstrom, T. Bringmann, M. Eriksson, and M. Gustafsson, Phys. Rev. Lett. **94**, 131301 (2005).
[37] H.-C. Cheng, J. L. Feng, and K. T. Matchev, Phys. Rev. Lett. **89**, 211301 (2002).
[38] C. Arina and N. Fornengo, J. High Energy Phys. 11 (2007) 029.
[39] D. Hooper and G. Servant, Astropart. Phys. **24**, 231 (2005).
[40] Y. Mambrini and C. Munoz, J. Cosmol. Astropart. Phys. 10 (2004) 003.
[41] V. Bertin, E. Nezri, and J. Orloff, Eur. Phys. J. C **26**, 111 (2002).
[42] E. A. Baltz, J. Edsjo, K. Freese, and P. Gondolo, Phys. Rev. D **65**, 063511 (2002).
[43] M. Gustafsson, E. Lundstrom, L. Bergstrom, and J. Edsjo, Phys. Rev. Lett. **99**, 041301 (2007).
[44] M. Perelstein and A. Spray, Phys. Rev. D **75**, 083519 (2007).
[45] L. Lopez Honorez, E. Nezri, J. F. Oliver, and M. H. G. Tytgat, J. Cosmol. Astropart. Phys. 02 (2007) 028.
[46] S. Arrenberg, L. Baudis, K. Kong, K. T. Matchev, and J. Yoo, Phys. Rev. D **78**, 056002 (2008).
[47] G. Bélanger, O. Kittel, S. Kraml, H. U. Martyn, and A. Pukhov, Phys. Rev. D **78**, 015011 (2008).
[48] C. Balazs, M. S. Carena, A. Freitas, and C. E. M. Wagner, J. High Energy Phys. 06 (2007) 066.
[49] B. C. Allanach, K. Cranmer, C. G. Lester, and A. M. Weber, J. High Energy Phys. 08 (2007) 023.
[50] H.-C. Cheng, K. T. Matchev, and M. Schmaltz, Phys. Rev. D **66**, 056006 (2002).
[51] H. Baer, A. Mustafayev, S. Profumo, A. Belyaev, and X. Tata, J. High Energy Phys. 07 (2005) 065.
[52] J. R. Ellis, K. A. Olive, Y. Santoso, and V. C. Spanos, Phys. Rev. D **71**, 095007 (2005).
[53] R. L. Arnowitt, B. Dutta, B. Hu, and Y. Santoso, Phys. Lett. B **505**, 177 (2001).
[54] G. Bélanger, F. Boudjema, A. Cottrant, A. Pukhov, and A. Semenov, Nucl. Phys. **B706**, 411 (2005).
[55] A. Djouadi, M. Drees, and J. L. Kneur, J. High Energy Phys. 08 (2001) 055.
[56] M. E. Gomez, G. Lazarides, and C. Pallis, Phys. Rev. D **61**, 123512 (2000).
[57] S. Profumo and A. Provenza, J. Cosmol. Astropart. Phys. 12 (2006) 019.
[58] S. Matsumoto, T. Moroi, and K. Tobe, Phys. Rev. D **78**, 055018 (2008).
[59] B. C. Allanach, G. Bélanger, F. Boudjema, and A. Pukhov, J. High Energy Phys. 12 (2004)020.
[60] E. A. Baltz, M. Battaglia, M. Peskin, and T. Wizansky, Phys. Rev. D **74**, 103521 (2006).
[61] T. Moroi, Y. Shimizu, and A. Yotsuyanagi, Phys. Lett. B **625**, 79 (2005).
[62] (Atlas Collaboration) Report No. CERN-LHCC-99-15, Vol. 2.
[63] G. L. Bayatian *et al.*, J. Phys. G **34**, 995 (2007).
[64] H. Baer, A. Belyaev, T. Krupovnickas, and J. O'Farrill, J. Cosmol. Astropart. Phys. 08 (2004) 005.
[65] H. Baer, T. Krupovnickas, S. Profumo, and P. Ullio, J. High Energy Phys. 10 (2005) 020.
[66] J. L. Feng, K. T. Matchev, and F. Wilczek, Phys. Lett. B **482**, 388 (2000).
[67] J. Angle *et al.*, Phys. Rev. Lett.**100**, 021303 (2008).
[68] Z. Ahmed *et al.* (CDMS Collaboration), Phys. Rev. Lett. **102**, 011301 (2009).
[69] H. S. Lee *et al.*, Phys. Rev. Lett. **99**, 091301 (2007).
[70] J. Angle *et al.*, Phys. Rev. Lett. **101**, 091301 (2008).
[71] S. Desai *et al.* (Super-Kamiokande Collaboration), Phys. Rev. D **70**, 083523 (2004); **70**, 109901(E) (2004).
[72] R. Bernabei *et al.* (DAMA Collaboration), Eur. Phys. J. C **56**, 333 (2008).
[73] F. Petriello and K. M. Zurek, arXiv:0808.2464.
[74] M. Y. Khlopov and C. Kouvaris, Phys. Rev. D **78**, 065040 (2008).
[75] D. R. Tovey, R. J. Gaitskell, P. Gondolo, Y. Ramachers, and L. Roszkowski, Phys. Lett. B **488**, 17 (2000).
[76] F. Giuliani and T. A. Girard, Phys. Rev. D **71**, 123503 (2005).
[77] F. Giuliani, Phys. Rev. Lett. **95**, 101301 (2005).
[78] H. Kraus *et al.*, J. Phys. Conf. Ser. **39**, 139 (2006).
[79] J. Collar *et al.*, Report No. FERMILAB-PROPOSAL-0961.
[80] V. K. Oikonomou, J. D. Vergados, and Ch. C. Moustakidis, Nucl. Phys. **B773**, 19 (2007).
[81] D. Hooper and G. Zaharijas, Phys. Rev. D **75**, 035010 (2007).
[82] V. Barger, W. Y. Keung, and G. Shaughnessy, Phys. Rev. D **78**, 056007 (2008).
[83] G. Bertone, D. G. Cerdeno, J. I. Collar, and B. C. Odom, Phys. Rev. Lett. **99**, 151301 (2007).
[84] G. Bélanger, F. Boudjema, A. Pukhov, and A. Semenov, arXiv:0803.2360.
[85] A. Bottino, F. Donato, N. Fornengo, and S. Scopel, Astropart. Phys. **18**, 205 (2002).
[86] G. Jungman, M. Kamionkowski, and K. Griest, Phys. Rep. **267**, 195 (1996).
[87] V. A. Bednyakov and F. Simkovic, Phys. Part. Nucl. **37**, S106 (2006).
[88] J. L. Bourjaily and G. L. Kane, arXiv:hep-ph/0501262.
[89] F. Giuliani, Phys. Rev. Lett. **93**, 161301 (2004).
[90] A. M. Green, J. Cosmol. Astropart. Phys. 08 (2007) 022.

[91] M. Drees and C.-L. Shan, J. Cosmol. Astropart. Phys. 06 (2008) 012.
[92] T. Falk, K. A. Olive, and M. Srednicki, Phys. Lett. B **339**, 248 (1994).
[93] (Atlas Collaboration) CERN-LHCC-99-14, Vol. 1.
[94] P. Skands *et al.*, J. High Energy Phys. 07 (2004) 036.
[95] K. Agashe and G. Servant, J. Cosmol. Astropart. Phys. 02 (2005) 002.
[96] G. Bélanger, A. Pukhov, and G. Servant, J. Cosmol. Astropart. Phys. 01 (2008) 009.
[97] B. A. Dobrescu, D. Hooper, K. Kong, and R. Mahbubani, J. Cosmol. Astropart. Phys. 10 (2007) 012.
[98] H.-C. Cheng and I. Low, J. High Energy Phys. 09 (2003) 051.
[99] H.-C. Cheng and I. Low, J. High Energy Phys. 08 (2004) 061.
[100] G. Bélanger, F. Boudjema, A. Pukhov, and A. Semenov, Comput. Phys. Commun. **176**, 367 (2007).
[101] G. Bélanger, F. Boudjema, A. Pukhov, and A. Semenov, Comput. Phys. Commun. **174**, 577 (2006).
[102] J. Hamann, S. Hannestad, M. S. Sloth, and Y. Y. Wong, Phys. Rev. D **75**, 023522 (2007).
[103] M. Kakizaki, S. Matsumoto, and M. Senami, Phys. Rev. D **74**, 023504 (2006).
[104] M. Kakizaki, S. Matsumoto, Y. Sato, and M. Senami, Phys. Rev. D **71**, 123522 (2005).
[105] T. Appelquist and H.-U. Yee, Phys. Rev. D **67**, 055002 (2003).
[106] R. S. Chivukula, D. A. Dicus, H.-J. He, and S. Nandi, Phys. Lett. B **562**, 109 (2003).
[107] The CalCHEP model file for the MUED model is available at http://home.fnal.gov/~kckong/mued/.
[108] A. Belyaev, C.-R. Chen, K. Tobe, and C. P. Yuan, Phys. Rev. D **74**, 115020 (2006).
[109] M. S. Carena, J. Hubisz, M. Perelstein, and P. Verdier, Phys. Rev. D **75**, 091701 (2007).
[110] A. Datta, K. Kong, and K. T. Matchev, Phys. Rev. D **72**, 096006 (2005).